Noise-induced dynamics in the mixed-feedback-loop network motif

Difei Li and Chunguang Li*
Centre for Nonlinear and Complex Systems, School of Electronic Engineering, University of Electronic Science and Technology of China, Chengdu 610054, People's Republic of China
(Received 6 July 2007; published 7 January 2008)

In this paper, we present a stochastic model for the mixed-feedback loop (MFL), a motif found in integrated cellular networks of transcription regulation and protein-protein interaction. Previous bifurcation analysis indicates that this motif can serve as a bistable switch or a clock. We investigate how extrinsic and intrinsic noise affects its dynamic behaviors systematically. We find that this motif can exploit noise to enrich its dynamical performance. When the MFL is in the bistable region, under fluctuation of extrinsic noise, the MFL system can switch from one steady state to the other and meanwhile one protein's production is amplified for more than three orders of magnitude. Further, from an engineering perspective, this noise-based switch and amplifier for gene expression is very easy to control. Without extrinsic noise, spontaneous transition between states occurs as the consequence of intrinsic noise. Such a switch is controlled by the parameters and system size. On the other hand, intrinsic noise can induce sustained stochastic oscillation when the corresponding deterministic system does not oscillate. Such stochastic oscillation shows the best performance at an optimal noise level, indicating the occurrence of intrinsic noise stochastic resonance which can contribute to the robustness of this oscillator. When considering the effects of extrinsic noise near bifurcation points, a similar phenomenon of extrinsic noise stochastic resonance is unveiled.

DOI: 10.1103/PhysRevE.77.011903 PACS number(s): 87.17.Aa, 87.16.Yc, 82.40.Bj

I. INTRODUCTION

Cells continuously sense their environment and generate appropriate responses. At the heart of this functionality are the interaction networks, or webs, of biochemical molecules, such as genes, proteins, and metabolites. The structures of a great deal of such networks, including networks of protein-protein interactions and transcription-regulatory networks, have been revealed after the development of high-throughput data-collection technologies. A major challenge in the post-genomic era is to quantitatively understand topological and dynamical properties and functions of these complex biological networks that control cellular functions [1].

Intensive statistical analysis on the transcriptional networks, consisting solely of transcription factors and their target genes, in *E. coli* and *S. cerevisiae* [2,3] have revealed significantly recurring nontrivial patterns of interconnections termed "network motif" contained in these networks. Later mathematical and experimental research suggests that motifs found in the transcriptional networks do perform specific information processing roles [4]. Moreover, it is found that, in many systems studied so far, the motifs are linked to each other in a way that does not spoil the independent function of each motif [5]. That means the network dynamics might be understood as combinations of these elementary computational units [6].

At the same time, statistical analysis of networks of protein-protein interactions in *S. cerevisiae* [7] also shows these networks comprising clusters of interacting proteins. Yet, some important information for a full description of cellular functions might be lost when transcriptional networks and networks of protein-protein interactions are separately analyzed, because in cells these two kinds of networks always work collaboratively rather than independently.

Recently, the concept of network motifs has been extended to include two types of interactions [8]: those between transcription factors and their target genes and those between proteins. The simplest such motif found in yeast *S. cerevisiae* is the two-nodes mixed-feedback loop (MFL) comprising one protein-protein interaction edge and one transcriptional-regulatory edge. In this motif, as shown in Fig. 1, protein A regulates gene b, and directly interacts with the product of gene b, protein B. In parallel, the MFL has been independently obtained as the core motif of several networks produced in an evolutionary procedure *in silico* aiming at creating small gene networks performing specific functions [9]. To better understand the dynamic properties of this simple genetic circuit, a mathematic model of the MFL based on the simplest biochemical interactions was proposed (see Ref. [10] for details about the biological processes in the MFL). This model will be described in the next section. The analysis of this model in detail reveals that there exist wide ranges of kinetic parameters where the MFL behaves either as a bistable switch or as an oscillator depending on whether gene b is repressed or activated by protein A.

Though the differential rate equations approach is widely used, its usefulness is limited when random fluctuations, or noise, in the systems interesting us cannot be ignored, which is always the case in biochemical processes, such as transcription and translation. Noise in biological networks arises

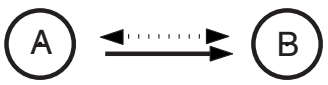

FIG. 1. MFL's architecture [8]. The dotted line represents the protein-protein interaction and the solid line represents the transcription regulation interaction.

*cgli@uestc.edu.cn

in two ways. *Intrinsic* noise originates from the stochastic nature of biochemical reactions that constitute the network. Its magnitude is proportional to the inverse of the system size. On the other hand, *extrinsic* noise originates from the random variation of one or more control parameters in the network, such as the rate constant of the transcription of a specific gene [11].

Lots of theoretical as well as experimental studies [11–21] have been carried out on the consequence of stochasticity in biological systems. These researches concerning noise in biological systems improve our understanding of real life processes. Stochasticity rooted in biochemical reactions can give rise to phenotypic variations even in clonal cell populations under the most uniform experimental conditions [16]. Organisms exploit this mechanism to achieve diversity and increase the likelihood of species survival over a wide range of environments. In addition, optimal intrinsic noise effects have been reported in some subcellular systems. For example, optimal intracellular calcium signaling appears at a certain size or distribution of the ion channel clusters [17]. In the circadian clock system and the calcium signaling system, when the system size is small and intrinsic noise must be considered, stochastic oscillations can be observed in a parameter region where the corresponding deterministic model only yields steady state. Such oscillations show the best performance at an optimal noise intensity, or an optimal system size [18,19]. For extrinsic noise, it has been demonstrated that in a bistable system derived from bacteriophage λ, an extrinsic noise source can be used as a switch and/or amplifier for gene expression which could have important implications for gene therapy [11]. Noise can also have significant effects on the stability and synchronization of genetic networks [20,21]. In this paper, we present the stochastic version model for the MFL and consider how extrinsic and intrinsic noise affects its dynamic behaviors.

II. STOCHASTIC MODELS OF MFL

A. Deterministic model for MFL

The MFL consists of two genes, a, b, and their products, protein A, B. Protein A regulates the transcription of gene b, and also directly interacts with protein B to form a dimer. To simplify the analysis, we adopted some reasonable assumptions, including that B does not interact with a protein A that is bound to gene b's promoter and the dimerization between protein A and B is irreversible. The time evolution of the number of the species in the MFL can be represented by the following four deterministic rate equations [10]:

$$\frac{d[b]}{dt} = \theta(1-[b]) - \alpha[b][A], \tag{1}$$

$$\frac{d[M_b]}{dt} = k_f[b] + k_b(1-[b]) - \upsilon_{M_b}[M_b], \tag{2}$$

$$\frac{d[A]}{dt} = \rho_A - k_{AB}[A][B] - \upsilon_A[A] + \theta(1-[b]) - \alpha[b][A], \tag{3}$$

$$\frac{d[B]}{dt} = k_B[M_b] - k_{AB}[A][B] - \upsilon_B[B]. \tag{4}$$

In these equations $[b]$, $[M_b]$, $[A]$, $[B]$ denote, respectively, the average number of free gene b, the mRNA of gene b, and the protein A and B per cell over a cell population. In our model and simulation next, we suppose that there is only a single gene b copy per cell. Therefore $[b]$ can also be seen as the probability that gene b is free without A bound to its promoter. Specifically, protein A binds to the b's promoter at a rate α and they dissociate at a rate θ. mRNA M_b is produced at a rate k_b when A binds to gene b or at a rate k_f otherwise. The production of protein A is assumed to be unregulated and at a given rate ρ_A. Without regulation, the transcripts of gene a quickly reach the steady state, therefore a separate description of a's transcription and translation is not needed in the deterministic model. The mRNA M_b produces protein B at a rate k_B. Protein A forms a dimer with B at a rate k_{AB} only when A does not bind to gene b. υ_M, υ_A, υ_B are the degradation rates for M_b, A, and B, respectively.

A detailed bifurcation analysis of this system showed that the behavior of the MFL depends on whether protein A is a transcriptional activator or a transcriptional repressor [10]. By analyzing the corresponding dimensionless form of these four rate equations, François *et al.* found that the bifurcation parameters are the two strengths of B protein production, k_Bk_f/υ_M and k_Bk_b/υ_M, when A is bound or not bound to the promoter of gene b, as compared to the production rate ρ_A of protein A. As in Ref. [10], we define $\rho_0=k_Bk_f/(\upsilon_M\rho_A)$ and $\rho_1=k_Bk_b/(\upsilon_M\rho_A)$. When A is a transcriptional repressor, i.e., $\rho_1<1<\rho_0$, two stable steady states can coexist: the number of protein A is high and that of B is low, or the number of protein B is high and that of A is low. A and B cannot both exist at a large amount. For instance, if A proteins are at a larger amount than B proteins, all B quickly associate with A and only free A and AB dimers remain. Free A binds to the promoter of gene b and represses the further production of protein B. On the other hand, when A is a transcriptional activator, i.e., $\rho_0<1<\rho_1$, the complexation of B with A acts as a negative feedback which makes oscillation possible. Besides, the MFL can have only one stable steady state in which $[A]$ is large when $\rho_0<1$ and $\rho_1<1$ or $[B]$ is large when $\rho_0>1$ and $\rho_1>1$.

Though deterministic rate equations are powerful tools for analyzing dynamical behaviors of both natural and artificial systems, they become insufficient for accurately describing the time evolution of species when noise in such systems cannot be ignored. There are two sources of noise in biological systems; *intrinsic* noise and *extrinsic* noise. Different mathematic descriptions are applied to account for them.

B. Extrinsic noise model for MFL

The two transcription rates of gene b, k_b and k_f, determine the dynamics of the MFL through the bifurcation parameters, ρ_0, ρ_1. Although the transcription is described as a single biochemical reaction in our model, it in fact consists of many sequential reactions. It is natural to assume that this part of the gene regulatory sequence is likely to be affected by fluc-

TABLE I. Reactions and corresponding transition rates in the model. Ω has the unit of a volume and can be seen as the system size.

Reaction	Description	Transition rate
$b+A \rightarrow bA$	protein A bound to the promoter of gene b	$W_1=r_1\Omega=\alpha[b]A$
$bA \rightarrow b+A$	protein A released from the promoter of gene b	$W_2=r_2\Omega=\theta(1-[b])\Omega$
$bA \rightarrow M_b+bA$	transcription of gene b with A bound to it	$W_3=r_3\Omega=k_b(1-[b])\Omega$
$b \rightarrow M_b+b$	transcription of gene b without A bound to it	$W_4=r_4\Omega=k_f[b]\Omega$
$M_b \rightarrow$	degradation of mRNA M_b	$W_5=r_5\Omega=\upsilon_M M_b$
$a \rightarrow M_a+a$	transcription of gene a	$W_6=r_6\Omega=k_a\Omega$
$M_a \rightarrow$	degradation of mRNA M_a	$W_7=r_7\Omega=\upsilon_{M_a}M_a$
$M_a \rightarrow A+M_a$	translation of mRNA M_a into protein A	$W_8=r_8\Omega=k_A M_a$
$A+B \rightarrow AB$	dimerization between protein A and B	$W_9=r_9\Omega=\frac{k_{AB}AB}{\Omega}$
$A \rightarrow$	degradation of protein A	$W_{10}=r_{10}\Omega=\upsilon_A A$
$M_b \rightarrow B+M_b$	translation of mRNA M_b into protein B	$W_{11}=r_{11}\Omega=k_B M_b$
$B \rightarrow$	degradation of protein B	$W_{12}=r_{12}\Omega=\upsilon_B B$

tuations of many internal or external parameters and it is interesting to consider the effect of such noise on the dynamics of the MFL. We vary the transcription rates by allowing the parameters k_b and k_f to vary stochastically, i.e., we set $k_b \rightarrow k_b+\xi(t)$ and $k_f \rightarrow k_f+\xi(t)$. The aforementioned model can be easily generalized to account for such extrinsic noise by altering Eq. (2): when k_b is fluctuated,

$$\frac{d[M_b]}{dt} = k_f[b] + k_b(1-[b]) - \upsilon_M[M_b] + \xi(t)(1-[b]), \tag{5}$$

and when k_f is fluctuated,

$$\frac{d[M_b]}{dt} = k_f[b] + k_b(1-[b]) - \upsilon_M[M_b] + \xi(t))[b], \tag{6}$$

where $\xi(t)$ is a rapidly fluctuating random term with zero mean $\langle\xi(t)\rangle=0$, and "δ-correlated" $\langle\xi(t)\xi(t')\rangle=D\delta(t-t')$. D is proportional to the strength of the perturbation. We simulate the extrinsic stochastic model by using the Euler-Maruyama scheme [22].

C. Intrinsic noise model for MFL

On the other hand, to account for intrinsic noise arising from the limited number of molecules participating in the molecular mechanism, one can describe the reaction system as a birth-death stochastic process governed by a chemical master equation (CME) which gives the time evolution of the probability distribution for the number of every species in the system [23]. Generally, the CME is hard to solve analytically. Instead, there have been a large number of *exact* or *approximate* numerical simulation methods [24–26] to generate trajectories of discrete, stochastic systems. Most of them are based on the exact algorithm introduced by Gillespie [24], which is rigorously equivalent to the CME. The stochastic version of the deterministic MFL model accounting for intrinsic noise is presented in Table I. The parameter Ω represents the system size and permits the modulation of the number of the molecules in the system [23]. Since the fluctuation in mRNA molecules' abundance is the major source of the intrinsic noise in gene expression [12], unlike the previous deterministic model, the transcription of gene a should be explicitly incorporated in the stochastic version model.

Though the exact Gillespie algorithm is widely used to study the consequence of intrinsic noise in many systems, it is computationally intensive when there are many molecules and reaction events. This limitation makes it hardly applicable when large system size is considered. To solve this problem, Gillespie introduced a τ-leap method [27] which randomly determines how many steps will take place for each reaction channel in the next "macroinfinitesimal" time interval. It has been proved that this method can produce significant gains in simulation speed with acceptable losses in accuracy when the system size is large. Therefore in our stochastic simulation, we use the exact method for small system size and the τ-leap method for large one.

Furthermore, when macroinfinitesimal time scales exist in the system, an approximate time-evolution equation of the Langevin type, termed chemical Langevin equation (CLE) can be applied [28,18]. For the present model, the CLE reads

$$\frac{d[b]}{dt} = r_2 - r_1 + \frac{1}{\sqrt{\Omega}}[\sqrt{r_2}\xi_2(t) - \sqrt{r_1}\xi_1(t)], \tag{7}$$

$$\frac{d[M_b]}{dt} = r_3 + r_4 - r_5 + \frac{1}{\sqrt{\Omega}}[\sqrt{r_3}\xi_3(t) + \sqrt{r_4}\xi_4(t) - \sqrt{r_5}\xi_5(t)], \tag{8}$$

$$\frac{d[M_a]}{dt} = r_6 - r_7 + \frac{1}{\sqrt{\Omega}}[\sqrt{r_6}\xi_6(t) - \sqrt{r_7}\xi_6(7)], \tag{9}$$

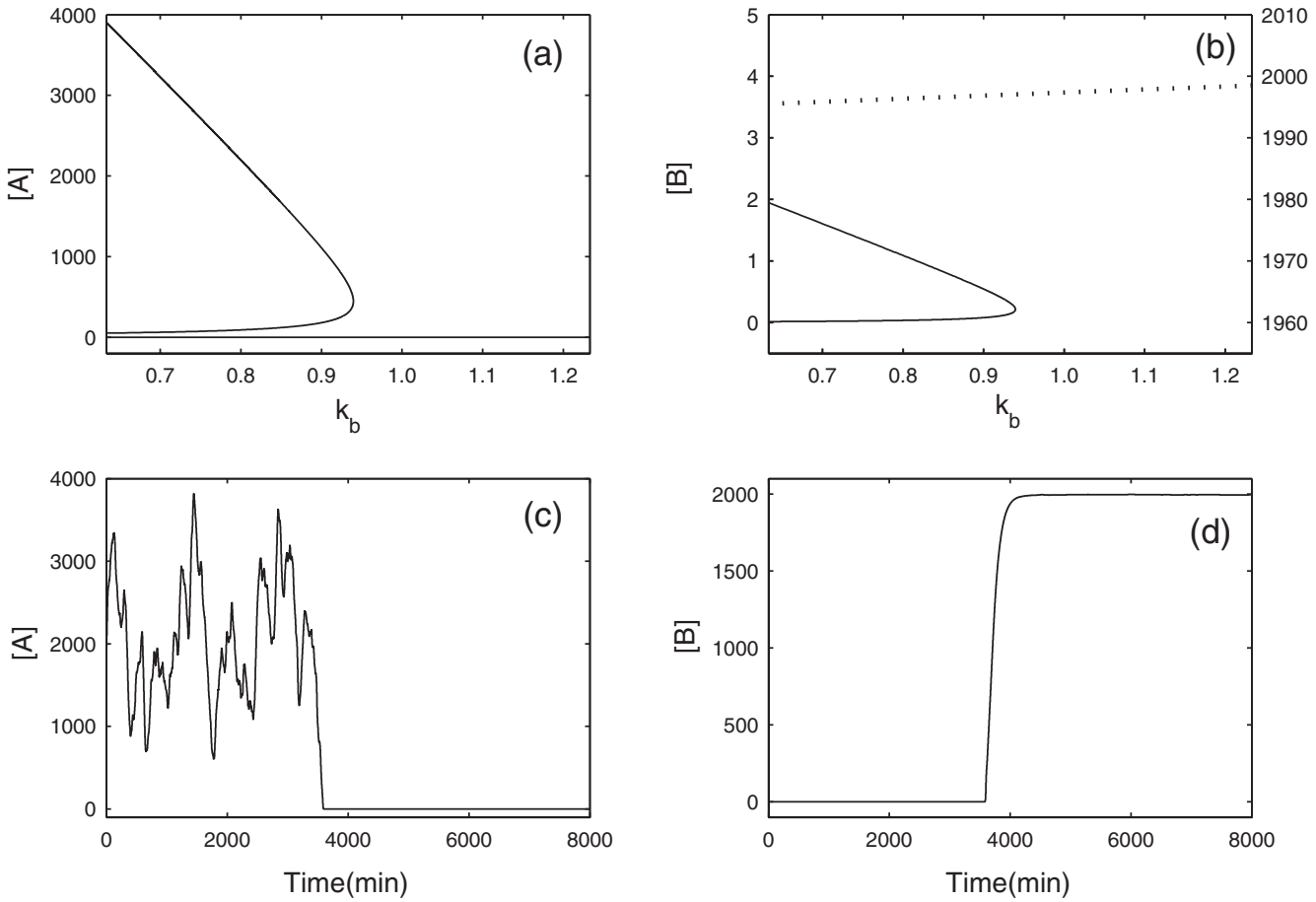

FIG. 2. Results for extrinsic noise affecting k_b with parameter values $k_b=0.8$ mol min^{-1}, $k_f=1.2$ mol min^{-1}, $D=1.5$. (a) Bifurcation diagram for the number of protein A vs k_b. (b) Bifurcation diagram for the number of protein B vs k_b. The steady state with a large number of B is plotted in the dotted line and corresponds to the right Y axis. The other two states are in the solid line and correspond to the left Y axis. (c) Time evolution for protein A. (d) Time evolution for protein B. Other parameters are $\theta=0.0399$ min^{-1}, $\alpha=0.001$ mol^{-1} min^{-1}, $v_{M_b}=0.03$ min^{-1}, $\rho_A=100$ mol min^{-1}, $k_{AB}=1$ mol^{-1} min^{-1}, $v_A=v_B=0.01$ min^{-1}, $k_B=3$ min^{-1}, where "mol" stands for molecules and "min" for minutes. Here and in the following figures, if not explicitly specified, these parameters are fixed. Data in (c) and (d) are obtained by simulating the extrinsic noise model with the Euler-Maruyama scheme.

$$\frac{d[A]}{dt} = r_8 - r_9 - r_{10} + r_2 - r_1 + \frac{1}{\sqrt{\Omega}}[\sqrt{r_8}\xi_8(t) - \sqrt{r_9}\xi_9(t) - \sqrt{r_{10}}\xi_{10}(t) + \sqrt{r_2}\xi_2(t) - \sqrt{r_1}\xi_1(t)], \tag{10}$$

$$\frac{d[B]}{dt} = r_{11} - r_9 - r_{12} + \frac{1}{\sqrt{\Omega}}[\sqrt{r_{11}}\xi_{11}(t) - \sqrt{r_9}\xi_9(t) - \sqrt{r_{12}}\xi_{12}(t)]. \tag{11}$$

Here, r_1-r_{12} are the transition rates per cell listed in Table I, and $\xi_1-\xi_{12}$ are Gaussian white noise with zero mean $\langle\xi_i(t)\rangle=0$ and correlation of $\langle\xi_i(t)\xi_j(t')\rangle=\delta_{ij}\delta(t-t')$. The transcription of gene a is also explicitly described. It is clear from the CLE that the magnitude of intrinsic noise is proportional to $\frac{1}{\sqrt{\Omega}}$ and depends on the dynamics of the MFL. To study the consequence of intrinsic noise without changing the deterministic kinetics, in the present work, we change the magnitude of the noise via the change of Ω. We will mainly use the CLE method in our simulation for convenience.

III. RESULTS

A. Extrinsic noise-induced switching and amplifying

As we have mentioned, two stable steady states of the MFL coexist when $\rho_1<1<\rho_0$, i.e., protein A is a transcription repressor. In the absence of noise, the number of the two proteins, A and B, in the MFL will evolve to one of the two fixed points completely determined by the initial state of the system. If we consider that extrinsic noise affects the two transcription rates of gene b, k_f and k_b, while keeping other parameters unaffected, novel behaviors come out.

Qualitatively, we can use the bifurcation plot to anticipate the effect of allowing the parameter to fluctuate. In Figs. 2(a) and 2(b), the steady state values of the concentration of proteins A and B for different values of parameter k_b are plotted. The system undergoes a saddle-node bifurcation at $k_b \approx 0.9396$ mol min^{-1} ($k_f=1.2$ mol min^{-1} and kept unchanged) and after that can only have one steady state with a small number of protein A and a large number of protein B. By comparing Figs. 2(a) and 2(b), we can anticipate that when the system is in the bistable region and has a large number of

A and a small number of B, if the parameter k_b varies, the change in the number of protein A will be dramatically large because of the steep top branch in Fig. 2(a), while the flat lower branch in Fig. 2(b) implies small variations in the number of protein B. But if the system stays at the other steady state in which there is a large number of B, only a mild change in both the number of proteins B and A occurs because of the flat lower branch in Fig. 2(a) and the flat top dotted branch in Fig. 2(b).

Next we incorporate extrinsic noise to make k_b stochastically vary and study the temporal behavior of the system under fluctuation. We simulated the extrinsic noise stochastic model for the MFL described in the previous section [Eqs. (1) and (3)–(5)] with large noise strength, $D=1.5$. Initially, the system is in the bistable region ($k_b=0.8$ mol min^{-1}, $k_f=1.2$ mol min^{-1}) beginning with the number of protein A equal to its upper value of approximately 2000 and protein B concentration about 0. The results are represented in Figs. 2(c) and 2(d). In the first instance, the fluctuation in the number of A is quite large while the number of B is nearly unchanged as we expected. Then, at around 4000 min, the number of protein A quickly drops to the lower value. Correspondingly, the number of protein B soon increases to its upper value and stays there with quite small variations. This phenomenon indicates that the extrinsic noise applied to the transcription rate k_b is sufficient to drive the system switching from one steady state to the other (across the unstable steady state). This transition is caused by the fast dimerization between proteins A and B. When the number of protein A is randomly fluctuated to a comparable value with that of B, most of the A quickly form a dimer with B, leaving the gene b unregulated. Then the number of protein B soon builds up to a rather high level if k_f is large enough.

A large fluctuation in the number of protein A before the switching indicates that the amount of this protein is quite sensitive to the variation in k_b if much more protein A exists in the system than protein B. But after the fast state switch at around 4000 min, flat curves in both Figs. 2(c) and 2(d) imply that the other steady state is nearly unaffected by the fluctuation in the value of k_b and is impossible to switch back if noise strength does not increase. That is to say, dynamical behaviors of MFL can be either sensitive or robust to the same perturbation affecting k_b depending on the specific state in which the MFL lies [29] and under such perturbation with large enough strength, MFL is very likely to switch to or stay at the robust state with a large number of B but quite a few A. We should also notice that in the fast switch, the number of protein B increases abruptly by over three orders of magnitude in a very short time if k_f is large enough. This feature indicates that the extrinsic noise affecting k_b might be used to amplify protein B's production.

Similar results can be obtained for the extrinsic noise affecting k_f except that the state which is sensitive to the fluctuation in k_b discussed above is robust to the random variation of k_f and the other state that is robust to the fluctuation in k_b is sensitive to the random variation of k_f. Therefore if the MFL is affected by the perturbation affecting k_f, contrary to the result when we consider fluctuation in k_b, the MFL is very likely to switch to or stay at the state with a large number of protein A but quite a few B. This interesting character of MFL allows us to obtain the desired state switch and amplifying in MFL easily by choosing the appropriate extrinsic noise source without the need to consider accurately tuning the strength and timing of noise as has been done in Ref. [11].

B. Spontaneous switching

Using the exact simulation method for the chemical reaction system [24], we also investigate the impacts of intrinsic noise on MFL when it is bistable. From Figs. 3 and 5, it is clear that if the small-size effect is taken into account, switching between states occurs spontaneously. The spontaneous switching observed is highly affected by two factors: the bifurcation parameter and the system size.

On one hand, the value of the bifurcation parameter determines whether MFL could act as a switch. We fix one of the two bifurcation parameters, k_f, and let k_b vary but always keep the MFL in the bistable region. We found that when k_b is too close to or too far away from the bifurcation point, MFL cannot act as a switch but prefers one of its two stable steady states under the fluctuation of the intrinsic noise. In Fig. 3, when $k_b=0.6$ mol min^{-1} (top panel), which makes MFL deep in the bistable region, MFL spends most of the time on the state with a large number of protein A. Though MFL can switch to the other state with lots of B, such a switch is quite rare and if that happens, the system will quickly switch back to the previous state with many protein A (data not shown). When $k_b=0.9$ mol min^{-1} (bottom panel in Fig. 3), which is close to the bifurcation point of the system, the state with a large number of B is preferred and MFL spends most of the time on this state.

We study quantitatively how k_b affects the ratio between the time MFL spends on the state with lots of protein A and the total time we simulate the chemical reactions in the MFL. The result is shown in Fig. 4. As k_b gets closer to the bifurcation point, MFL spends less time on the state with large number of A. Only when k_b is around 0.8 mol min^{-1}, the time MFL spends on its two steady states is nearly equally distributed. Otherwise, MFL will prefer one of its two stable steady state, and spend most of the time dwelling on this preferred state. In other words, when intrinsic noise is considered, only when k_b is around 0.8 mol min^{-1}, MFL keeps the bistability predicted in the deterministic model. When k_b is away from this value, MFL tends to be monostable.

On the other hand, the system size of MFL determines the stability of the spontaneous switch, which is a widely known result on stochastic switch. As the system size increases, the stability of the spontaneous switch is enhanced and characteristic switching time increases drastically, which can be seen from Fig. 5. When the systems size increases, the number of the more abundant protein will be concentrated around the value predicted in the deterministic model and seldom fluctuated to a small enough value which makes state switch possible.

We also study the effect of k_{AB}, the rate of the dimerization between A and B on the spontaneous switch and in the parameter region we considered, there is no obvious correlation between k_{AB} and the performance of the switch.

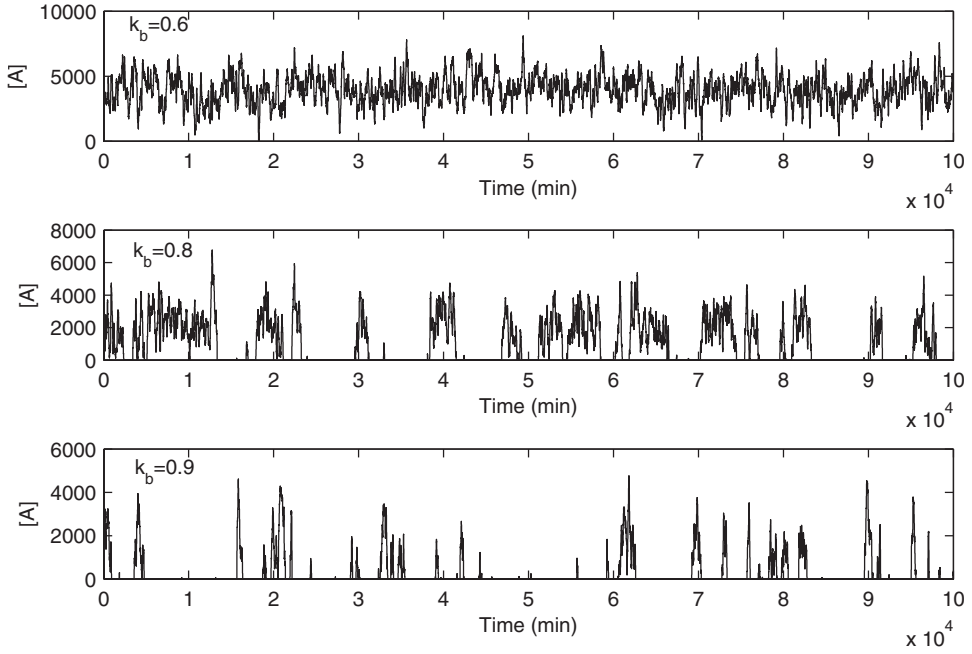

FIG. 3. Effect of k_b on the switch of MFL. Time series for the number of protein A are shown. From top to the bottom, $k_b = 0.6, 0.8, 0.9$ mol min^{-1}, respectively, $k_f = 1.2$ mol min^{-1}, $\Omega = 1$. Because of the small size considered here, data in Figs. 3–5 are obtained by using the exact Gillespie algorithm.

In our simulation, the two factors, the bifurcation parameter and the system size, affect different aspects of the performance of MFL when it acts as a genetic switch. Such difference may imply that when we try to characterize a genetic switch, these two factors should be both considered.

C. Intrinsic noise stochastic resonance

Besides the bistable region, the MFL can sustainedly oscillate if $\rho_0 < 1 < \rho_1$, i.e., protein A is a transcription activator. The MFL is a simple genetic network that can oscillate without some specific features, such as additional positive feedback loop or the self-activation of gene a, required in some other biological oscillators [10]. The effect of intrinsic noise on variety of genetic oscillators has been widely studied. For a circadian clock deep inside the oscillation region, it is well known that if intrinsic noise resulting from small system size has been taken into account, the oscillations will be no longer correlate in time [30,31]. In this case, intrinsic noise plays a destructive role. However, as the authors stated in Ref. [31], if the circadian clock is tuned nearly to the Hopf bifurcation point, such a conclusion fails. Therefore it is interesting for us to consider the effect of intrinsic noise in the MFL near the bifurcation point from monostable steady state to oscillation.

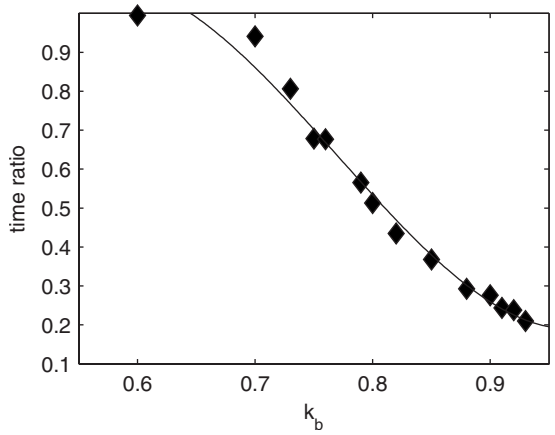

FIG. 4. Dependence of the ratio between the time MFL spends on the state with lots of protein A and the total time we simulate the chemical reactions in the MFL on k_b(mol min^{-1}). Solid line: cubic data fitting.

For the MFL system, when $k_f = 0.5$ mol min^{-1} and k_b mol min^{-1} varies, other parameters as listed in Fig. 2, the system undergoes a supercritical Hopf bifurcation at $k_b \approx 1.247$ mol min^{-1}. In the present work, we focus on the effect of the intrinsic noise when k_b is tuned closed to this bifurcation point. The following simulations are based on the intrinsic noise model for MFL in the previous section (Table I).

If $k_b < 1.247$ mol min^{-1}, the MFL can only display damped oscillation and approach its stable steady state asymptotically when intrinsic noise is ignored. But if we consider small size effect, simulations via the exact method and the τ-leap method both reveal the sustained stochastic oscillation [Fig. 6(a)]. The number of the species in the MFL would not reach the steady state predicted in the differential equations but oscillates with uncertain periods and amplitudes. Interestingly, this type of uncertainty is distinct from random noise since there are clear peaks in the power spectrums [Fig. 6(b)]. In Fig. 6(b), the power spectrum density (PSD) for the stochastic oscillation of the transcripts of gene b under three different system sizes are plotted. The control parameter is $k_b = 1.24$ mol min^{-1} which is slightly less than

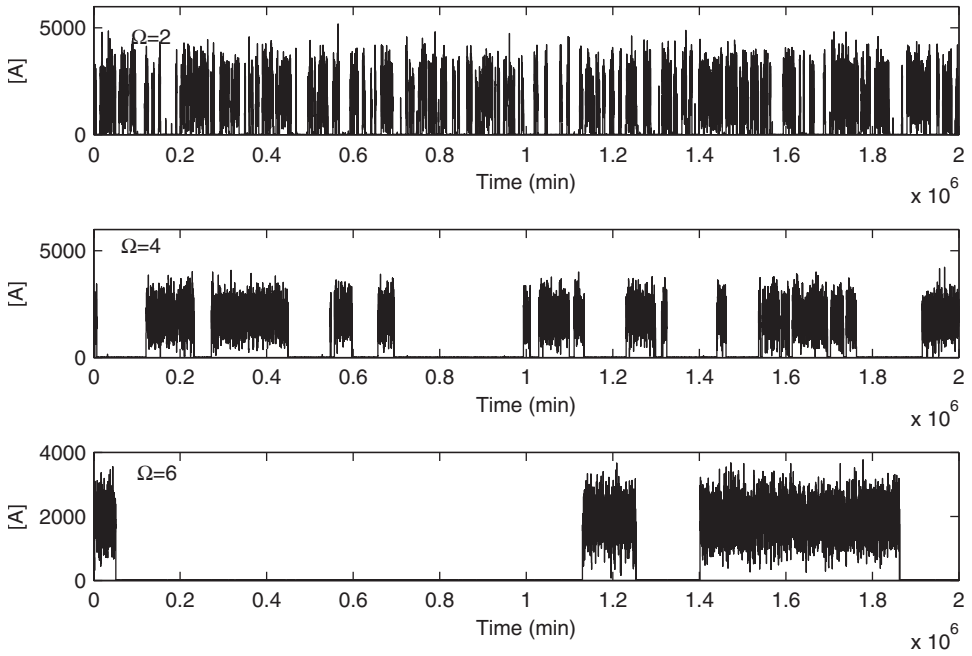

FIG. 5. Effect of system size Ω on the switch of MFL. Time series for the number of protein A are shown. From top to the bottom, $\Omega=2,4,6$, respectively, $k_b=0.8$ mol min^{-1}, $k_f=1.2$ mol min^{-1}.

the bifurcation value. The time series used to calculate the power spectra contains 14 500 data points with an average time interval of 1 min. The smoothed curves are obtained by nearest averaging over 40 points from the original one. Clear peaks appear on all of the three curves, which implies that the time series contain periodic information or the system dynamics generates coherent motion [32]. When the system size increases from 10 to 10^5, both the signal level and noise background decrease at the peak. For an intermediate system size $\Omega=10^3$, the peak is the most pronounced among the three. This indicates that the stochastic oscillation caused by intrinsic noise shows some kind of coherent resonance with the deterministic dynamics in MFL [18,33].

The mechanism for such coherent resonance can be explained qualitatively by studying the effect of noise strength on both the amplitude and period of the stochastic oscillations [Fig. 6(a)]. When $\Omega=10$, sustained stochastic oscillation would be overwhelmed by the intrinsic noise. Therefore both the amplitude and period of the stochastic oscillation are quite irregular and consequently both the height and the width of the peak on the curve for $\Omega=10$ in Fig. 6(b) are larger than those for the other two system sizes. As system size increases, noise strength decreases. As a result, the amplitude of oscillations tends to be more concentrated around the steady state predicted in the deterministic differential equations and the height of the peak on the PSD curve would also decrease. Meanwhile, the oscillation period would be more regular and lead to that the characteristic frequency of the stochastic oscillation gets closer to the frequency of the deterministic oscillation which occurs when k_b is slightly larger than the bifurcation value and noise effect is ignored, and correspondingly, the peak on PSD curves becomes narrower [the curves in Fig. 6(b) for $\Omega=10^3$ and $\Omega=10^5$]. Only at optimal noise level, $\Omega=10^3$, is the peak most pronounced.

To measure the relative performance of the stochastic oscillations quantitatively, an effective signal-to-noise ratio β is defined as in [18], $\beta=[P(\omega_p)/P(\omega_2)]/(\Delta\omega/\omega_p)$, where ω_p is the frequency at the peak and $P(\cdot)$ indicates the power spectrum density at a given frequency. $\Delta\omega=\omega_1-\omega_p$, where ω_1 satisfies $\omega_1>\omega_p$, and $P(\omega_1)=P(\omega_p)/e$ with e as the base of the natural logarithm. $P(\omega_2)$ is the smallest PSD value between $P(0)$ and $P(\omega_p)$. For example, the SNR β for the curve of $\Omega=10^3$ in Fig. 6(b) can be calculated as follows: $\beta=[P(B)/P(A)]/[(\omega_C-\omega_B]/\omega_B)$, $P(C)=P(B)/e$. The dependence of β on system size for $k_b=1.24$ mol min^{-1} is plotted in Fig. 7(a). We can see that a clear maximum is presented for system size $\Omega=10^3$, which demonstrates the existence of a resonance effect. This resonance effect is completely induced by the intrinsic noise, so it is called intrinsic noise stochastic resonance (INSR) [18].

We also simulate the intrinsic noise model for MFL using the CLE method when the system size $\Omega\geqslant 100$ (when the system size is small, the conditions for using the CLE are not satisfied). From Fig. 7(a), the good qualitative agreement among the exact method, the τ-leap method, and the CLE method allows us to use the CLE for convenience. Using CLE, we have also studied how the INSR behavior depends on the value of the control parameter. The result is shown in Fig. 7(b). When the control parameter k_b gets closer to the bifurcation value, both the maximum SNR and the optimal size become larger. For k_b slightly larger than the bifurcation value, the peak disappears and the SNR monotonically increases with the increment of system size.

How do living organisms use INSR to function is still an open question. We conjecture that INSR is a mechanism to enhance the robustness of biological oscillators. In small system size, which is always true in biological systems, the MFL sustainedly oscillates in a much larger parameter region than expected in the corresponding deterministic system. The system size at which the SNR curve (Fig. 7) reaches the maximum can be seen as a critical value. When the size of

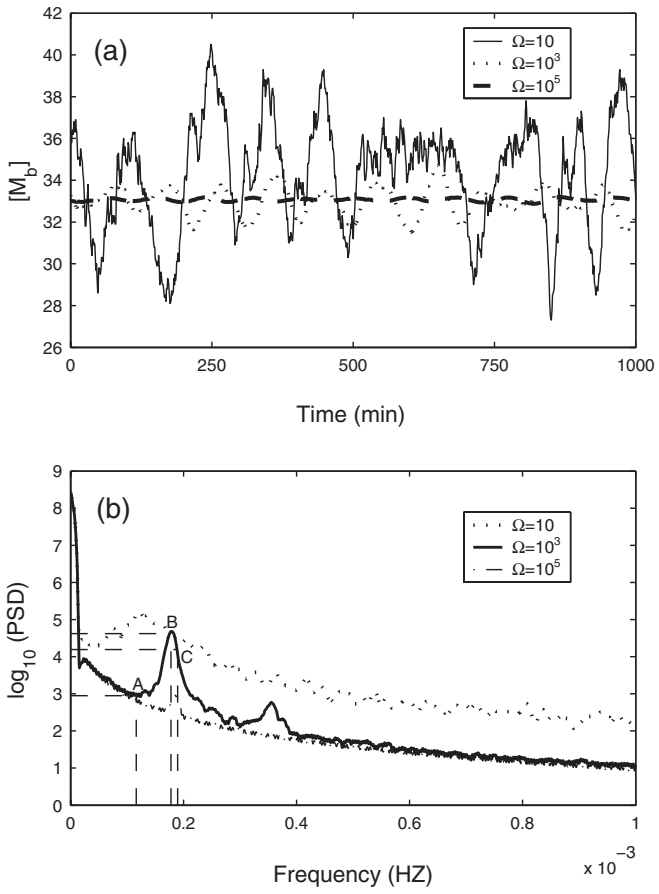

FIG. 6. (a) Time series for the transcripts of gene b: M_b for $\Omega=10$, $\Omega=10^3$, $\Omega=10^5$. (b) Smoothed power specta for the intrinsic noise-induced stochastic oscillation of M_b for $\Omega=10$, 10^3, and 10^5. The control parameter is $k_b=1.24$ mol min^{-1}. The curve for $\Omega=10$ is obtained from the exact simulation method while the other two are from the τ-leap method. On the curve for $\Omega=10^3$, point B corresponds to the peak, point A corresponds to the smallest PSD in the frequency range $[0,\omega_B]$, and at point C, $P(C)=P(B)/e$. The parameters $k_a=1$ mol min^{-1}, $v_{M_a}=0.03$ min^{-1}, $k_A=3$ min^{-1}, and the others are the same as those listed in the caption of Fig. 2.

the system is smaller than this critical value, the SNR for MFL with k_b above the supercritical Hopf bifurcation value and the SNR for MFL with k_b below this bifurcation value is of the same order and comparable. Since the SNR is calculated from the power spectrums which reflect the information about both the amplitude and period of the stochastic oscillation, similar SNR values imply that the stochastic oscillations from which the SNR is calculated are similar in many aspects. The similarity between the stochastic oscillations when MFL is outside and inside the domain of deterministic oscillation could guarantee that the dynamical behaviors of MFL would not change dramatically and result in a disastrous consequence for the cell if some critical parameters are occasionally perturbed to a value below the bifurcation point. Only when the system size is larger than this critical value, the difference between the SNR values when MFL is outside and inside the domain of deterministic oscillation increases as the system size increases and, as a consequence, a small perturbation in the parameters around the bifurcation point would result in a big difference in the dynamical behaviors. However, from Fig. 7(b), we can also see that when the control parameter becomes further away from the bifurcation value, the critical value defined above becomes smaller, which means that this mechanism is not robust and would be ineffective if the perturbation of the control parameter is relatively large.

Another possible benefit of INSR for biological oscillators is that if the system size of these genetic networks with the module of MFL is near the critical value producing the maximum SNR, these systems fully exploit INSR to make the stochastic oscillations as regular as possible. It has been reported that in intracellular calcium signaling, similar coherent resonance is also observed and the realistic size of ion channel clusters is near the optimal value generating the best calcium signaling [17]. Direct experiments and measurements of cells containing a MFL module might help us determine whether in such systems SNR is always at the optimal value. Since the MFL has been found as a core module both in genetic networks in nature and the ones generated in computer-based evolution procedures, INSR may be a mechanism for robust functioning of the networks where the MFL is embedded.

D. Extrinsic noise stochastic resonance

Next we consider the effects of extrinsic noise on a current system near the Hopf bifurcation point. The extrinsic noise model for MFL proposed in Sec. II resembles nonlinear systems perturbed by noise without extrinsic periodic force once considered in [32]. However, in [32], noise enters the dynamic system additively, i.e., $\dot{x}=f(x)+\xi(t)$ while in our model, extrinsic noise in MFL is multiplicative, i.e., $\dot{x}=f(x)+g(x)\xi(t)$, and therefore is directly coupled with the dynamics of MFL. It has been found that under fluctuation of additive noise, stochastic resonance (SR) occurs in autonomous nonlinear systems, i.e., SR without extrinsic signal [32]: Noise induces coherent motion in a system which will asymptotically approach the stable steady state if noise is absent and such coherent motion is most pronounced at optimal noise strength.

To explore the effects of extrinsic noise near the bifurcation point, we simulate the extrinsic noise model for MFL using the Euler-Maruyama method. First we set $k_b=1.24$ mol min^{-1}, which is slightly less than the Hopf bifurcation value and let k_b be fluctuated by extrinsic noise ($k_f=0.5$ mol min^{-1}). When the noise strength D is nonzero, MFL oscillates stochastically around the steady state predicted in the corresponding deterministic model. The fluctuation increases as the noise strength becomes larger. Surprisingly, as the results obtained above for intrinsic noise, the stochastic oscillation induced by extrinsic noise is also quite different from random noise. Clear peaks also appear on the power spectra for the stochastic oscillations of the transcripts of gene b (data not shown) and these peaks imply the existence of coherent motion in this system. Such coherent motion is most strong for an optimal noise strength and this means that extrinsic noise in MFL induces the SR phenomenon.

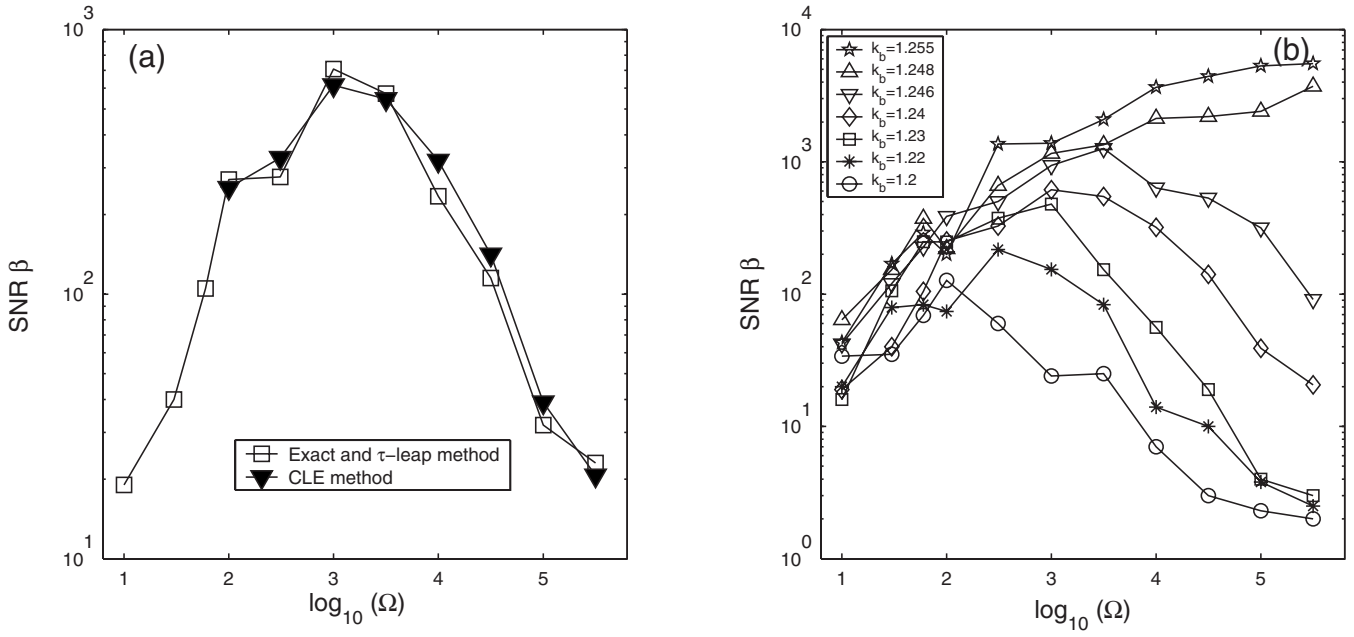

FIG. 7. (a) Dependence of the effective SNR on the system size for $k_b=1.24$ mol min^{-1}. Open squares: data obtained by the exact method when $\Omega<100$ and by the τ-leap method when $\Omega\geqslant 100$; solid triangles: data from CLE method. (b) Dependence of SNR on system size for different control parameter k_b. The data are obtained by the exact method when $\Omega<100$ and the CLE method once $\Omega\geqslant 100$.

Extrinsic noise stochastic resonance can be explained by the twofold role noise plays. On one hand, noise stimulates coherent motion in MFL; otherwise the system will approach the steady state asymptotically. On the other hand, noise spoils the coherent behaviors activated by itself. As a result, only at an optimal noise level, the competition of the two effects is balanced and the resonance can be observed.

We also calculate the effective signal-to-noise ratio (SNR) β to measure relative performance of the stochastic oscillations induced by extrinsic noise quantitatively. In Fig. 8(a), the dependence of SNR on strengths of extrinsic noise is plotted. When the control parameter k_b is less than the bifurcation value, the SNR curves all have a maximum which clearly illustrates the occurrence of stochastic resonance. The resonance observed here is completely induced by extrinsic noise, therefore we call it extrinsic noise stochastic resonance (ENSR). As k_b approaches the bifurcation value, the maximum of the SNR increases and the optimal noise

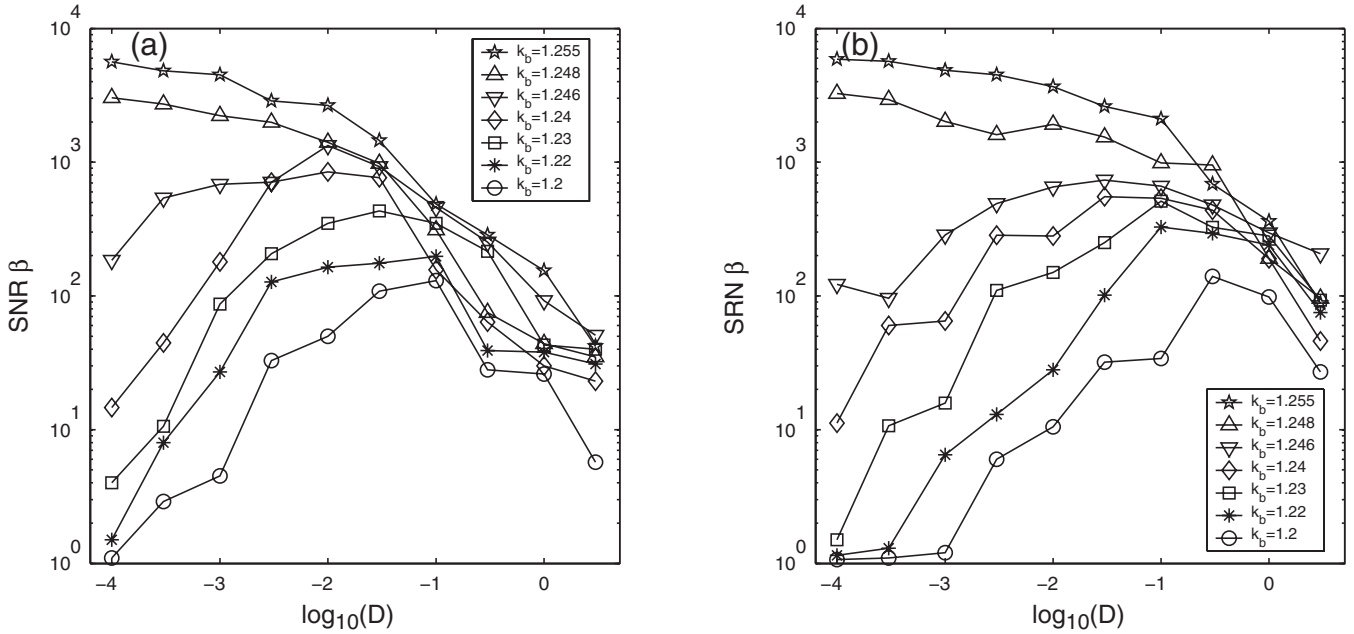

FIG. 8. (a) Dependence of SNR on strengths of extrinsic noise fluctuating k_b. (b) Dependence of SNR on strengths of extrinsic noise fluctuating k_f. In both (a) and (b), $k_f=0.5$ mol min^{-1}. Data in (a) and (b) are obtained by simulating the extrinsic model with the Euler-Maruyama scheme.

strength gets smaller. Once k_b is above the bifurcation value, ENSR disappears and SNR decreases monotonically as the noise strength becomes larger.

We also study the effects of extrinsic noise fluctuating k_f. When k_b is less than the bifurcation value, k_f is not a bifurcation parameter. In Fig. 8(b), the dependence of SNR on strengths of extrinsic noise fluctuating k_f is plotted. Similar stochastic resonance can also be seen clearly. There is no big qualitative difference between Figs. 8(a) and 8(b) so that we are firmly convinced that stochastic resonance is completely caused by extrinsic noise. However, the maximum of SNR for each k_b when extrinsic noise fluctuates k_b is larger than the corresponding one when k_f is fluctuated. This difference indicates that when extrinsic noise directly affects the bifurcation value, SR will do a better performance.

The similar effect of intrinsic and extrinsic noise on MFL when this system is near a Hopf-bifurcation point is to some extent unexpected since intrinsic noise, arising from small system size effect, affects every single biochemical reaction we listed in Table I directly and simultaneously, while extrinsic noise, arising from the perturbation of one parameter in MFL, only affects the transcription of gene *b* directly and then propagates to other components of this genetic network. The similarity between the shape of the curves describing the dependence of SNR on noise strength and between the value of the maximum on these curves may imply that at least from the aspect of stochastic resonance, though the sources of intrinsic and extrinsic noise are quite different, the effect of them on genetic oscillators cannot be well separated.

IV. DISCUSSION

Networks of biochemical molecules are responsible for the functionality of cells. But their intrinsic complexity inhibits us to understand them as a whole. Instead, researchers turn to study the building block, or motif, of these networks. Elucidating these motifs' dynamics and functions would shed light on the whole networks' behaviors. Computational models based on experimental data have been proven to be quite useful to solve these problems. Most of these models have the form of ordinary differential equations to describe the time evolution of the concentration of the biochemical species involved. But the noise from the environmental fluctuations or the stochastic nature of the biochemical reactions is unavoidable in biological systems. It is well known that noise can have great impacts on these systems' dynamical properties, for example, the robustness in circadian rhythm [34].

In the present work, we have built the stochastic models for the MFL, a motif found in integrated cellular networks of transcription regulation and protein-protein interaction, and study the effect of two sources of noise, *extrinsic* and *intrinsic*, on the dynamic behaviors of this motif. We found that if noise is considered, MFL generates some different phenomena not observed in the corresponding deterministic model.

When one protein in the MFL represses the production of the other one, two stable steady states coexist. In this case, extrinsic noise fluctuating the two transcription rates the repressed gene can induce quickly switch between the two steady states. Any one of the two steady states is sensitive to one type of the two different extrinsic noises but robust to the other. This feature makes this type of switch easy to control because carefully tuned noise strength is not needed. In the switching process, the concentration of the protein is quite low before the switch can be amplified by more than three orders of magnitude. For the effective genetic treatments of many diseases, the expression of a transfected gene needs to be regulated in some systematic fashion [11]. Therefore the development of extrinsically controllable noise-based switches and amplifiers for gene expression could have significant clinical implications and the MFL might be quite useful for that. To make this feature of MFL clinically applicable, it is important to look for an appropriate noise source. Sets of chemical reactions that affect the transcription of gene *b* might be used as the noise input of this switch.

For intrinsic noise, in a small area in the bistable region of MFL, bistability predicted in the deterministic model is maintained and MFL can act as a spontaneous genetic switch. The stability of such switching is determined by the system size. Outside this area, bistability of MFL is lost.

On the other hand, it was found that the intrinsic noise can induce sustained stochastic oscillation when the corresponding deterministic system only yields steady state. In addition, the performance of such oscillation approaches a maximum at an optimal noise intensity, indicating the occurrence of the intrinsic noise stochastic resonance, which has also been observed in circadian clock [18] and intracellular calcium oscillations [19]. We have argued that INSR might enhance the robustness of biological oscillators. However, due to the lack of biological data concerning dynamical behaviors of MFL, we cannot answer directly whether the size of real biological oscillators is always near the optimal value to make the mechanism of INSR fully exploited. For extrinsic noise, near the bifurcation point, the consequence of extrinsic noise is quite similar to that of the intrinsic noise and extrinsic noise stochastic resonance can be observed. Such similarity makes the difference between the effect of intrinsic and extrinsic noise on MFL unexpectedly vague.

An interesting feature of MFL is the coexistence of bistability and oscillation. In the deterministic model, there are clear borderlines among the monostable, bistable, and oscillation region. However, under the fluctuation of intrinsic noise, the borderline between the monostable and bistable region and the borderline between the monostable and oscillation region become vague. Meanwhile, the oscillation region is enlarged while the bistable region is reduced. It will be interesting to explore in future study whether this phenomenon implies that oscillation is preferred when bistability and oscillation are both present in a genetic network.

Since realistic genetic network examples of MFL are ubiquitous in nature, the noise-induced dynamic behaviors presented in our results may exist in many of them. Since simple genetic network motifs are always embedded in a larger and more complex network, under some circumstances, it might be not easy for us to observe *in vivo* the phenomena predicted here due to the fact that MFL no longer functions independently, but as pointed out in [5] in many cases the functions can be preserved.

ACKNOWLEDGMENTS

The authors sincerely thank Yigong Xiao, Wei Huang, and Feng Chen for insightful discussions. This work was supported by the National Natural Science Foundation of China (Grant No. 60502009), the Youth Foundation of Sichuan Province (Grant No. 07ZQ026-019), and the Program for New Century Excellent Talents in University (Grant No. NCET-05-0801). C.L. would also like to acknowledge support from the Alexander von Humboldt Foundation.

[1] S. A. Kauffman, *The Origins of Order* (Oxford University Press, New York, 1993); L. H. Hartwell, J. J. Hopfield, S. Leibler, and A. W. Murray, Nature (London) **402**, C47 (1999); A. L. Barabási and Z. N. Oltvai, Nat. Rev. Genet. **5**, 101 (2004).

[2] S. S. Shen-Orr, R. Milo, S. Mangan, and U. Alon, Nat. Genet. **31**, 64 (2002).

[3] R. Milo, S. S. Shen-Orr, S. Itzkovitz, N. Kashtan, D. Chklovskii, and U. Alon, Science **298**, 824 (2002).

[4] U. Alon, *An Introduction to System Biology: Design Principles of Biological Circuits* (Chapman and Hall, London, 2006); C. Li, L. Chen, and K. Aihara, IEEE Signal Process. Mag. **24**, 136 (2007).

[5] U. Alon, Nature (London) **446**, 497 (2007).

[6] R. J. Prill, P. A. Iglesias, and A. Levchenko, PLoS Biol. **3**(11), e343 (2005).

[7] S. Wuchty, Z. N. Oltvai, and A. L. Barabási, Nat. Genet. **1135**, 176 (2003).

[8] E. Yeger-Lotem, S. Sattath, N. Kashtan, S. Itzkovitz, R. Milo, R. Y. Pinter, U. Alon, and H. Margalit, Proc. Natl. Acad. Sci. U.S.A. **101**, 5934 (2004).

[9] P. François and V. Hakim, Proc. Natl. Acad. Sci. U.S.A. **101**, 580 (2004).

[10] P. François and V. Hakim, Phys. Rev. E **72**, 031908 (2005).

[11] J. Hasty, J. Pradines, M. Dolnik, and J. J. Collins, Proc. Natl. Acad. Sci. U.S.A. **97**, 2075 (2000).

[12] M. Kærn, T. C. Elston, W. J. Blake, and J. J. Collins, Nat. Rev. Genet. **6**, 451 (2005).

[13] P. B. Warren and P. R. ten Wolde, Phys. Rev. Lett. **92**, 128101 (2004).

[14] A. Lipshtat, A. Loinger, N. Q. Balaban, and O. Biham, Phys. Rev. Lett. **96**, 188101 (2006).

[15] R. J. Allen, P. B. Warren, and P. R. ten Wolde, Phys. Rev. Lett. **94**, 018104 (2005).

[16] H. H. McAdams and A. Arkin, Trends Genet. **15**, 65 (1999); G. M. Suel, J. Garcia-Ojalvo, L. M. Liberman, and M. B. Elowitz, Nature (London) **440**, 545 (2006).

[17] J. W. Shuai and P. Jung, Proc. Natl. Acad. Sci. U.S.A. **100**, 506 (2003).

[18] Z. Hou and H. Xin, J. Chem. Phys. **119**, 11508 (2003).

[19] H. Li, Z. Hou, and H. Xin, Phys. Rev. E **71**, 061916 (2005).

[20] C. Li, L. Chen, and K. Aihara, PLOS Comput. Biol. **2**(8), e103 (2006); L. Chen, R. Wang, T. Zhou, and K. Aihara, Bioinformatics **22**, 2722 (2005).

[21] C. Li, L. Chen, and K. Aihara, BMC Syst. Biol. **1**, 6 (2007); C. Li, L. Chen, and K. Aihara, IEEE Trans. Circuits Syst., II: Express Briefs **54**, 892 (2007).

[22] P. E. Kloeden, E. Platen, and H. Schurz, *Numerical Solution of SDE Through Computer Experiments* (Springer-Verlag, Berlin, 1994).

[23] N. G. Van Kampen, *Stochastic Processes in Physics and Chemistry* (North-Holland, Amsterdam, 1981).

[24] D. T. Gillespie, J. Chem. Phys. **81**, 2340 (1977).

[25] M. A. Gibson and J. Bruck, J. Phys. Chem. A **104**, 1876 (2000).

[26] E. L. Haseltine and J. B. Rawlings, J. Chem. Phys. **117**, 6959 (2002).

[27] D. T. Gillespie, J. Chem. Phys. **115**, 1716 (2001).

[28] D. T. Gillespie, J. Chem. Phys. **113**, 297 (2000).

[29] J. Stelling, U. Sauer, Z. Szallasi, F. J. Doyle, and J. Doyle, Cell **118**, 675 (2004).

[30] D. Gonze and A. Goldbeter, Chaos **16**, 026110 (2006).

[31] D. Gonze, J. Halloy, and P. Gaspard, J. Chem. Phys. **116**, 10997 (2002).

[32] Gang Hu, T. Ditzinger, C. Z. Ning, and H. Haken, Phys. Rev. Lett. **71**, 807 (1993).

[33] Z. Wang, Z. Hou, and H. Xin, Chem. Phys. Lett. **401**, 307 (2005).

[34] D. Gonze, J. Halloy, and A. Goldbeter, Proc. Natl. Acad. Sci. U.S.A. **99**, 673 (2002).